Ecological Indicators 144 (2022) 109519

Contents lists available at ScienceDirect

Ecological Indicators

journal homepage: www.elsevier.com/locate/ecolind

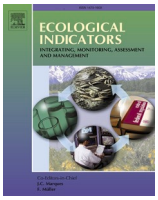

Original Articles

Remote sensing indicators to assess riparian vegetation and river ecosystem health

G. Pace [a,b,*], C. Gutiérrez-Cánovas [c], R. Henriques [d], C. Carvalho-Santos [a,b], F. Cássio [a,b], C. Pascoal [a,b]

[a] Centre of Molecular and Environmental Biology (CBMA), Department of Biology, University of Minho, Campus of Gualtar, 4710-057 Braga, Portugal
[b] Institute of Science and Innovation for Bio-Sustainability (IB-S), University of Minho, Campus of Gualtar, 4710-057 Braga, Portugal
[c] Biological Invasions group. Department of Integrative Ecology. Doñana Biological Station (EBD-CSIC). Av. Américo Vespucio, 26. Isla de la Cartuja. 41092 Seville, Spain
[d] Department of Earth Sciences, University of Minho, Institute of Earth Sciences (ICT), Campus of Gualtar, 4710-057 Braga, Portugal

ARTICLE INFO

Keywords:
Sentinel-2
Normalized Difference Vegetation Index
Land Use Intensification
Riparian buffer
Aquatic macrophytes
Anthropogenic pressures

ABSTRACT

Environmental managers need information to quickly detect which stressor combinations should be addressed to reverse river degradation across large study areas. The pivotal role of riparian vegetation in regulating thermal regimes and inputs of light, nutrients and organic matter has made it a major target of stressor-mitigation and conservation actions. However, due to the dendritic and extensive nature of river networks, field-based monitoring of local riparian conditions is expensive and time-consuming. Ongoing developments in remote sensing offer an unparalleled opportunity to address this challenge. Nonetheless, there is still a limited understanding of the capacity of remote sensing indicators to predict changes in local riparian and river conditions, urging for local calibration with *in situ* measurements. This study aims to evaluate the capacity of remote sensing to detect impacts on quality elements commonly used in river biomonitoring: riparian vegetation, abiotic river condition and macrophyte biomass. To this end, four remote sensing metrics were tested against field-based indicators in 50 stream locations from four river basins across the Northwest of Portugal: i) the lateral riparian continuity at reach scale (riparian forest buffer width), ii) the riparian vegetation density at reach scale (Normalized Difference Vegetation Index, $NDVI_{100m}$), and iii) the land use intensification at both reach (LUI_{100m}) and iv) segment (LUI_{500m}) scales. We found that the combination of remote sensing variables (riparian forest buffer width and the land use intensification index) correlated with riparian vegetation quality and dissolved inorganic nitrogen concentrations. We also found that the riparian vegetation density was able to predict changes in vascular plant biomass except for bryophytes. Our study provides new insights on the capacity of satellite-based indicators to assess riparian and river health, illustrating their utility for land and water managers, to identify and monitor, at a reduced cost and time, potential changes in the riparian vegetation.

1. Introduction

Human activities have produced multiple interacting pressures on river ecosystems, including land-use intensification and hydroclimatic alterations (Dudgeon et al., 2006; Reid et al., 2019). Despite increasing EU efforts to reverse freshwater degradation through Water Framework Directive, only 41 % of the European surface water bodies reached a good ecological status (EEA, 2018; Filipe et al., 2019). One major obstacle to restore ecological health is the accumulation of multiple stressors across spatial and temporal scales (Birk et al., 2020; Capon et al., 2021). Cumulative effects of multiple stressors produce cascading effects that undermine biodiversity and ecosystem functioning, and stand out as the main threat for riparian and aquatic ecosystems worldwide (Bruno et al., 2016). Therefore, there is a need to develop cost-effective indicators that help to identify which stressor combinations should be addressed to reverse river degradation and to ensure the long-term sustainability of river ecosystems (Carvalho et al., 2019).

The pivotal role of riparian vegetation in regulating thermal regimes and inputs of light, nutrient and organic matter (Yirigui et al., 2019; Riis et al., 2020), has made it an important target for stressor-mitigation or

* Corresponding author.
E-mail address: giorgio.pace@bio.uminho.pt (G. Pace).

https://doi.org/10.1016/j.ecolind.2022.109519
Received 12 May 2022; Received in revised form 13 September 2022; Accepted 28 September 2022
Available online 1 October 2022

biomonitoring actions (Feld et al., 2018). However, due to the dendritic and extensive nature of river networks, field-based monitoring of local riparian conditions is expensive and time-consuming. Ongoing developments in remote sensing offer an unparalleled opportunity to address this challenge. However, we have a limited understanding on the capacity of remote sensing variables to anticipate changes in local riparian and river conditions.

The use of satellite data has a great potential to increase both spatial coverage and the frequency of riparian and river monitoring (Huylenbroeck et al., 2020). For example, 2 m resolution multispectral WorldView-2 satellite images were used to discriminate exotic species (e.g., willow stands) from surrounding native riparian vegetation (Doody et al., 2014). Aerial LiDAR data were used to analyze forest conditions (height, longitudinal continuity, water accessibility) of riparian buffer to highlight their regional variability and explore the factors controlling it (Michez et al., 2017). In particular, the structure of riparian vegetation (i.e., density and complexity) was typically monitored by means of spectral indices to estimate the fraction of photosynthetically active radiation absorbed by Earth's vegetation and to map its distribution within the entire river networks (Novillo et al., 2019; Pérez-Silos et al., 2019). Among the high number of vegetation indices, the Normalized Difference Vegetation Index (NDVI) has been frequently used to assess large scale and long-term trends of vegetation (Peng et al., 2012). NDVI can be used to monitor primary productivity over time (Pace et al., 2021), to investigate productivity–diversity relationships (Wang et al., 2016; Torresani et al., 2019) and to determine vegetation and landscape structure (Álvarez-Martínez et al., 2018; Rocchini et al., 2018). In addition, multi-temporal remotely sensed vegetation indices can be used to detect changes in riparian areas and deltas due to hydrological and bioclimatic processes (e.g., floods and droughts; Nagler et al., 2020) or due to anthropogenic activities (e.g., dams and alteration of hydrologic and sediment regimes; Nagler et al., 2016; Zaimes et al., 2019). However, there is still uncertainty associated with the use of NDVI metrics in fluvial ecosystems. The high spatial heterogeneity of river landscape and the high temporal dynamics of river-corridor habitats may lead to contrasting outcomes between NDVI and field-based approaches, urging the need for a local calibration with *in situ* measurements (Bizzi et al., 2016; Knehtl et al., 2018; Fonseca et al., 2021; Dias-Silva et al., 2021).

Remote sensing has been also used to produce land use maps over large areas across ecosystems (Costa et al., 2018; Schulz et al., 2021). Recent advances in machine learning algorithms, together with the increased availability of dense time series data, have further enhanced the precision and the accuracy of land use mapping (Potapov et al., 2015; Holloway and Mengersen, 2018; Venter and Sydenham, 2021). Since streams are particularly sensitive to land use at local and catchment scales, land cover classes and land use indices (LUI) have been frequently used to assess, indirectly, the quality of stream water (Feld, 2004; Tran et al., 2010). However, the most adequate spatial scale to assess human influence on stream quality is still uncertain, because different scales (catchment scale, reach scale, local buffers, riparian corridors) can provide contrasting results (Fernandes et al., 2011; Monteagudo et al., 2012; Wahl et al., 2013; Erba et al., 2015).

In this context, remote sensing offers a promising avenue to predict local riparian and river conditions. For example, riparian density and lateral continuity are usually related to the amount of available habitat within the riparian zone, thus they are directly related to the riparian quality (Fonseca et al., 2021). On one hand, riparian density reflects how well riverbed is shadowed by vegetation, thus it mediates water temperature by intercepting solar radiation (Garner et al., 2017). On the other hand, riparian lateral continuity mediates the exchange of energy and materials with the surrounding landscape; thus, it can be directly related to the lateral inputs of nutrients (De Sosa et al., 2018). Moreover, disturbances in the major extension of the riparian ecosystem along the river margin (e.g. fragmentation and clearing) have direct effects on riverbank stabilization, thereby contributing to erosion and instream sedimentation (Tufekcioglu et al., 2020). As such, certain land use categories (e.g. agricultural or pasture land uses) may magnify deliveries of N or P into streams, thus landscape metrics can explain reach-scale impacts (Finkler et al., 2021; Lei et al., 2021).

In addition to that, riparian vegetation has an effect on freshwater habitats by influencing environmental conditions (Evangelista et al., 2017), and producing cascading effects on freshwater organisms. By intercepting light, nutrients and sediments, riparian trees are considered key environmental filters that can influence primary producers especially aquatic macrophytes (Baattrup-Pedersen et al., 2006; Tremp, 2007; Hrivnák et al., 2010; Jusik and Staniszewski, 2019). Therefore, remote sensing metrics that describe riparian density and lateral continuity may also serve as proxies of local abiotic conditions and aquatic primary producers (e.g., macrophye biomass).

This study aims to evaluate the capacity of remote sensing metrics to detect impacts on field-based quality elements commonly used in river biomonitoring, namely riparian vegetation, abiotic river condition and macrophyte biomass. Specifically, we determined i) the capacity and suitability of remote sensing variables to represent direct field observations, as well as their relationships with riparian quality, maximum water temperature, concentration of dissolved nutrients in stream water and percentage of instream fine sediments; and ii) the relative importance of remote sensing *versu* local abiotic variables to represent the observed spatial distribution in macrophyte biomass. To this end, we derived four remote sensing metrics characterizing the lateral riparian continuity at the reach scale (riparian forest buffer width), the riparian vegetation density at the reach scale (Normalized Difference Vegetation Index) and the land use intensification at the reach and the segment scales.

2. Materials and methods

2.1. Study area

We selected 50 stream reaches (some examples are in Fig. S1 as supplementary information) in four river basins across the Northwest of Portugal, the Minho, the Lima, the Cávado and the Ave River basins, which drain to the Atlantic Ocean (Fig. 1). The Minho River is an international water body of approximately 300 km. Its drainage basin covers 17,080 km^2 (Mota et al., 2014). The Lima River spring is in the San Mamede mountain (Spain) at an altitude of about 950 m. The total catchment area is 2535 km^2, from which more than half is in Spain (Santos et al., 2004). The Cávado River basin occupies 1,589 km^2, with a mean elevation of 564 m with several peaks of 1,500 m. The water is intensively used for hydropower generation, domestic and industrial water supply and agricultural irrigation (Vieira et al., 1998). The upper parts of these three basins are within the Peneda-Gerês National Park and contains river segments with species and habitats important for conservation. Concerning riparian vegetation, native broadleaved forests are dominated by the presence of *Quercus robur* and *Quercus pyrenaica f*ollowed by *Alnus glutinosa*, *Salix atrocinerea*, *Laurus nobilis and Crataegus monogyna*, which characterize the Galicio Portuguese oak woods (Habitat 9230 *sensu* Habitats Directive, European Commission, 1992; European Commission, 2013); *A. glutinosa*, *Fraxinus excelsior*, *Osmunda regalis* and *S. atrocinerea*, which characterize the Alluvial forests Osmundo-Alnion (Habitat 91E0 *sensu* Habitat Directive, European Commission, 1992; European Commission, 2013). Concerning aquatic macrophytes, the water courses are often characterized by the presence of submerged or floating vegetation (e.g., *Ranunculus fluitans, R. trichophyllus and* Callitriche spp.) or aquatic mosses (e.g., *Fontinalis antipyretica*), which are characteristic of the *Ranunculion fluitantis* and *Callitricho-Batrachion* vegetation (Habitat 3260 *sensu* Habitats Directive, European Commission, 1992; European Commission, 2013). Lastly, the Ave River spring is in the Cabreira mountain and it runs through ca. 94 km long, with an area of ca. 1,390 km^2 (Araujo et al., 1998). The water is intensively used for agriculture and industry.

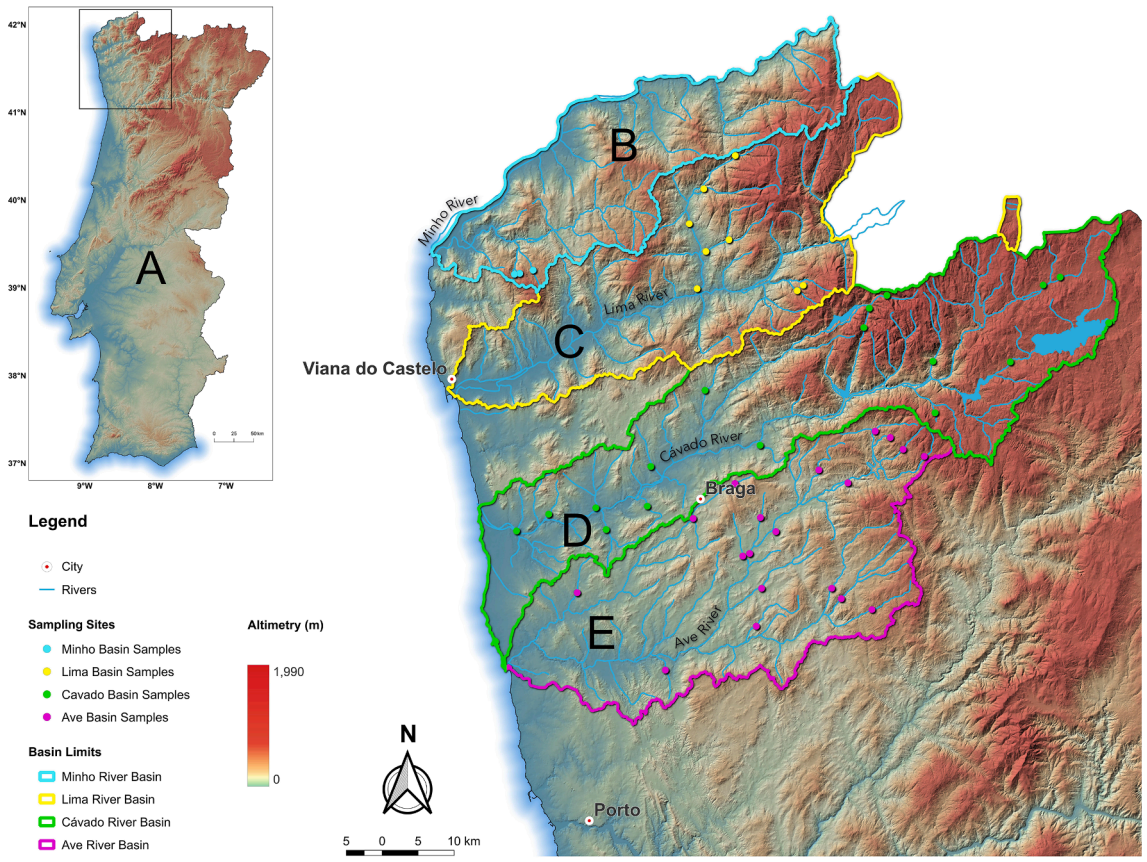

Fig. 1. (A) Map of Portugal with the distribution of the 50 stream reaches across four river basins; (B) Minho River Basin and sampling sites; (C) Lima River Basin and sampling sites; (D) Cávado River Basin and sampling sites; (E) Ave River Basin and sampling sites.

2.2. Remote sensing data

To characterize the riparian lateral continuity and density, we used Google Earth satellite's high-resolution images and Sentinel-2 orthorectified surface reflectance images (S2A MSI L2A). To cover the whole study area, we selected two scenes (T29TNG and T29TNF tiles), with the lowest amount of noise (e.g., shadows and clouds). The acquisition strategy was designed to meet fundamental quality standards, namely i) to have no cloud cover during summer months, ii) to minimize phenological variation (Zaimes et al., 2019), iii) to get the highest riparian vegetation complexity corresponding to the most productive time for riparian vegetation in our study area (Pace et al., 2021), iv) to get the highest vegetation expansion, according to the soil moisture content and the phreatic water table depth, during baseflow conditions (Gurnell et al., 2001) and v) to match our field data (June 2020). Images were acquired from Copernicus Open Access Hub user interface, developed by the European Space Agency for Earth observation. Sentinel-2 images were chosen since they offer freely available high spatial resolution images (10 m to 20 m) and multi-spectral global coverage.

To characterize land use intensification at the local scale, we used the Portuguese Land Use and Land Cover map also known as COS (https://www.dgterritorio.pt). COS is a vectorial map with a minimum mapping unit of one hectare and offers a detailed level of thematic and positional accuracy. This map is harmonized with global and European policies

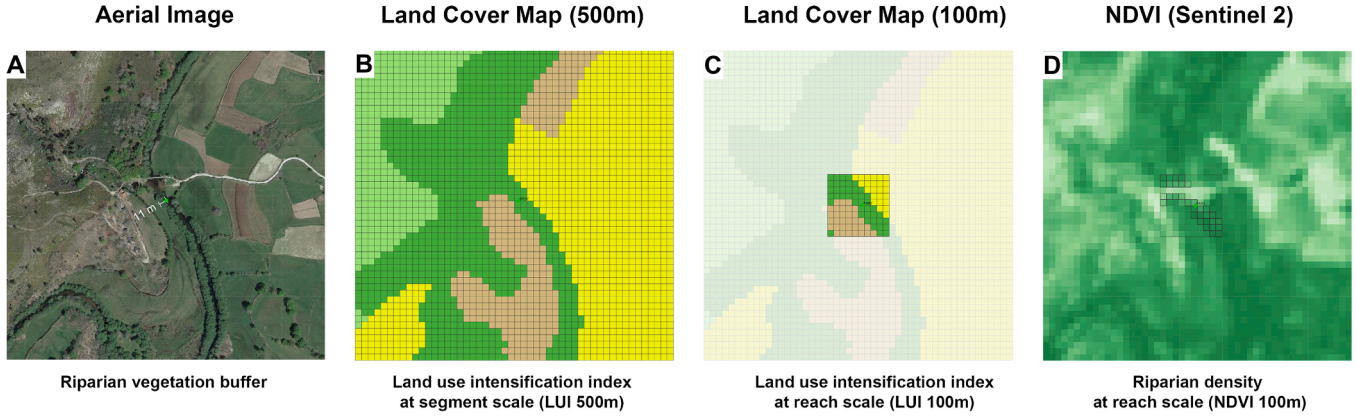

Fig. 2. Research approach for the remote sensing indicators retrieval: (A) the riparian forest buffer width (BUFF); (B) the land use intensification index at the segment scale (LUI_{500m}); (C) the land use intensification index at the reach scale (LUI_{100m}); (D) the riparian density at reach scale (NDVI100m): mean NDVI values were calculated only for pure riparian pixels (black squares).

related to geographic data quality and standards (Costa et al., 2018).

2.2.1. Computation of remote sensing metrics

Based on Google Earth satellite's high-resolution images, S2A MSI L2A images and COS layers, four remote sensing metrics were calculated (Fig. 2): 1) the width of the riparian vegetation buffer (BUFF), which reflects the lateral continuity of the riparian vegetation in both streambanks; 2) the Normalized Difference Vegetation Index of the riparian vegetation ($NDVI_{100m}$), which provides a proxy of riparian vegetation density at the reach scale; 3) the land use intensification index for fine grain (LUI_{100m}), which indicate local landscape intensification at the reach scale; and 4) the land use intensification index for coarse grain (LUI_{500m}), which indicate landscape intensification at the segment scale that includes agricultural activities that generate pollutants, nutrient enrichment and sedimentation.

We calculated a riparian forest buffer width (BUFF) at each sampling site using Google Earth satellite's high-resolution images, loaded in QGIS via the QuickMapServices plugin. Width was calculated for both bank sides. Then, we calculated the averaged bank side values to have a representative site-specific value.

Land use intensification indexes (LUI) were calculated as in Eq. (1) through a weighted mean which considers land-use categories and their percentage of occupation using the scoring system outlined by Feld (2004) and applied by Erba et al. (2015).

$LUI = 5\ (\%artificial) + 3\ (\%agricultural) + (\%pasture)$ (1).

We derived two land use intensification indexes at different grain sizes for the reach and the segment scale, respectively: 100 × 100 m (LUI_{100m}) or 500 × 500 m (LUI_{500m}) cells.

The Normalized Difference Vegetation Index (NDVI) was calculated for all images acquired as per Eq. (2) using bands 4 and 8 in Sentinel-2, which have been calibrated to measure radiation in the visible (Red) and near-infrared (NIR) regions of the spectrum, respectively.

$NDVI = (NIR\text{-}RED)/(NIR + RED)$ (2).

NDVI values range between − 1.0 and 1.0, with values close to 1 indicating more greenness and vegetation activity. NDVI values nearing zero and below indicate non-vegetated areas (e.g., water, snow, ice, clouds and barren surfaces). To estimate the riparian vegetation density at the reach scale, we first identified the number of riparian vegetation pixels (each pixel had a 10 m spatial dimension) within a 100 × 100 m cells. Riparian vegetation pixels, included in the land cover class of riparian forests and shrubs, were identified based on COS layers and Google Earth high resolution maps. Then, we estimated the mean NDVI values belonging to the riparian vegetation identified. Finally, we multiplied the mean NDVI values obtained by the percentage of riparian vegetation pixels within the 100x100m cells. In this way, we restricted our NDVI analysis only to pure riparian vegetation pixels avoiding noise from mixed pixel due to agriculture and urban land cover (e.g. crops, parks) in the site-specific floodplains. Some representative photos from the field and satellite (Google Earth satellite's high-resolution images and NDVI maps) of the riparian areas monitored in our study are in Fig. S1.

All spatial analyses were performed in QGIS 3.10.12 (Quantum GIS Development Team, 2009).

2.3. Characterization of instream condition

We surveyed the 50 stream reaches (approximately 100-m reach) in two consecutive years (2019 and 2020) during summer (July and September). These reaches were characterized based on their chemical condition, vegetation structure, habitat complexity and hydrological condition, using classical *in situ* methodologies at one sampling site for each reach as follow.

At each sampling site, stream water samples were collected into plastic bottles, transported in a cool box (4 °C) to the laboratory and used within 24 h for chemical analyses. Concentrations of phosphate, nitrite, nitrate, and ammonium were determined using a HACH DR/2000 spectrophotometer (Hach Company, Loveland, CO, USA). Total dissolved inorganic nitrogen (DIN) was calculated as the sum of nitrite, nitrate and ammonium concentrations. For each sampling site, dissolved oxygen and water temperature were recorded every 10 min during 24 h using PME-miniDo$_2$T Logger. These dataloggers were fixed to the river bed at 10–30 cm depth within 0.5 m from the stream margin using iron bars. This information was used to calculate maximum daily temperature for each site.

For each sampling site, relative light levels were measured for 30 days using Onset- HOBO UA-002–64 dataloggers. We also estimated the percentage of stream channel shading by direct *in situ* observation.

Riparian vegetation structure and ecological quality were evaluated based on the riparian quality index (QBR; Munné et al., 2003). The QBR focuses on the riparian areas with an emphasis on the total riparian cover, the cover structure, the cover quality and the anthropogenic alteration (Zaimes and Iakovoglou, 2021). Habitat complexity was evaluated based on the habitat hetereogeneity index (IHF; Pardo et al., 2002), whereas the percentage of fine sediments was estimated visually. Mean current velocity was derived by averaging between 5 and 15 measurements (depending on the channel width) of a flow meter (Valeport Electromagnetic Flow Meter-Model 801). Results of instream condition measures are in Table S1.

2.4. Macrophyte sampling and biomass determination

For each site, macrophyte cover and biomass were surveyed along 40-m reach following the national protocols (INAG, 2008). We defined macrophytes as any vascular plant or bryophyte growing in the stream channel or directly at the water-land interface. Each reach was visually divided into three sectors and the frequency of occurrence for each macrophyte type (aquatic vascular plant or bryophyte) was estimated by counting the squares of occurrence (Rääpysjärvi et al., 2016). For each sector and date, we collected one sample of aquatic vascular plants and bryophytes with a quadrat of 0.01 m^2 surface. Chlorophyll-*a* concentration in macrophyte tissues was determined by spectrophotometry, following extraction in 90 % acetone (Jeffrey and Humphrey, 1975). We estimated aquatic vascular plant and bryophyte biomass as their Chlorophyll-*a* concentration per unit of surface at the reach scale. To do this, the mean Chlorophyll-*a* concentration from up to three samples of vascular plants and bryophytes was determined and multiplied by their reach-scale cover.

2.5. Data analysis

First, we used Pearson's correlation coefficients to explore the capacity of remote sensing metrics (BUFF, $NDVI_{100m}$, LUI_{100m}, LUI_{500m}) to depict riparian and instream habitat features ($n = 50$; dataset from 2020). Response variables were the riparian quality index, the percentage of stream channel shading, the maximum water daily temperature, the percentage of fine sediments, and the concentration of dissolved inorganic nitrogen (DIN) and soluble reactive phosphorus (SRP). Next, to understand which combinations of remote sensing predictors better capture variations in riparian and instream habitat features, we adopted a multi-model inference approach based on linear regression models (Burnham and Anderson, 2002; Grueber et al., 2011). To do this, for each response variable, we evaluated the explanatory capacity of seven linear regression models considering all possible combinations of predictors, excluding those with high collinearity (Zuur et al., 2009). Thus, we avoided models including $NDVI_{100m}$, LUI_{100m}, LUI_{500m} simultaneously, because they showed high collinearity (Variance Inflation Factor, VIF > 2). Afterwards, using the *dredge*() function from the MuMIn R package (Barton, 2020), we ranked all seven models using the values of the Akaike Information Criterion for small sample sizes (AICc) and retained those models with $\Delta AICc \leq 7$ relative to the model ranked first (Zuur et al., 2010). For each model, we also derived the explained variance (R^2) and Akaike weights to inform on the

explanatory power and the relative likelihood of each model of being the best model. We used the MuMIn R package to calculate AICc, rank models and estimate explained variance and Akaike weights (Barton, 2020). For the retained models (best models), based on model's Akaike weights, we finally obtained the mean-weighted partitioned variance for each predictor (Hoffman and Schadt, 2016). To better understand the association between remote sensing metrics and field measures (riparian and instream habitat features), we calculated the normalized root-mean squared error (nRMSE) of each model from a 5-fold cross-validation process using *cv.lmvar*() function from the lmvar R package (Partners, 2019). Cross-validations were performed using untransformed response variables to allow comparisons across models (Rääpysjärvi et al., 2016).

To evaluate the capacity of remote sensing *versu* abiotic instream features to represent the observed spatial distribution in macrophyte biomasses we followed a similar approach (i.e., correlations plus multi-model inference) ($n = 100$; datasets from 2019 and 2020). In this case, we used linear mixed-effect models to account for repeated measures in the same site for consecutive years. In brief, for each response variable, we evaluated 15 mixed-effect models including all possible combinations of remote sensing and instream abiotic predictors, avoiding those combinations with high collinearity (i.e., excluding predictor combinations meeting VIF > 2). Then, following the procedure explained above, we ranked models based on AICc values, obtained predictor coefficients, explained variance for each predictor and Akaike weights, and retained best models (ΔAICc ≤ 7).

For all models, residuals plots were visually checked to verify model assumptions. Before analysis and to reduce distribution skewness, we performed a log-transformation for river width, riparian forest buffer widths, relative light levels and concentrations of soluble reactive phosphorus. We performed a square-root transformation for Chlorophyll-*a* content, the land use intensification index at both reach and segment scales, altitude, maximum temperature, dissolved inorganic nitrogen and mean current velocity. We performed a logit transformation for the NDVI values, percentage of stream channel shading and the riparian quality index. Finally, we z-standardized (mean = 0, SD = 1) predictors to facilitate comparisons among model coefficients. All statistical analyses were executed in R 3.5.1 (R Core Team, 2020).

3. Results

3.1. Associations between remote sensing metrics, riparian quality and instream conditions

The riparian vegetation density ($NDVI_{100m}$) and the riparian forest buffer width (BUFF) were positively correlated with the riparian quality index ($r_P = 0.72$ for both cases; Fig. 3), whereas this index showed a negative relationship with land use intensification at reach and segment scales (r_P = -0.75 for LUI_{100m} and r_P = -0.69 for LUI_{500m}; Fig. 3). Conversely, $NDVI_{100m}$ and BUFF were negatively correlated with dissolved inorganic nitrogen concentrations (DIN) (r_P = -0.67 and −0.59 respectively; Fig. 3) and soluble reactive phosphorus concentration (SRP) ($r_P = -0.40$ and −0.43 respectively; Fig. 3). LUI indices displayed a positive correlation ($r_P = 0.70$) with DIN (Fig. 3), SRP ($r_P = 0.44$; Fig. 3) and the percentage of fine sediments ($r_P = 0.61$ for LUI_{100m} and $r_P = 0.57$ for LUI_{500m}; Fig. 3). BUFF was the only variable showing a positive correlation with river shadow ($r_P = 0.33$; Fig. 3), whereas LUI_{500m} was the only one that presented a significant positive correlation with the maximum daily temperature ($r_P = 0.33$; Fig. 3).

The relative contribution of remote sensing metrics to each riparian and instream conditions varied considerably across features (Fig. 4). LUI_{100m} was generally the best predictor of riparian quality index (mean explained variance: 41.2 %, nRMSE = 0.34) followed by LUI_{500m} (mean explained variance: 13 %, nRMSE = 0.39) and BUFF (mean explained variance: 12.3 %, nRMSE = 0.38). BUFF was the best predictor of channel shading (mean explained variance: 19 %, nRMSE = 0.69), followed by $NDVI_{100m}$ (mean explained variance: 0.01 %, nRMSE = 0.64) and LUI_{100m} (mean explained variance: 0.01 %, nRMSE = 0.69). Maximum daily temperature was best explained by LUI_{500m} (mean explained variance: 12.3 %, nRMSE = 0.13). The percentage of fine sediments was best explained by LUI_{100m} (mean explained variance: 31.7 %, nRMSE = 0.61) followed by LUI_{500m} (mean explained variance: 5.2 %, nRMSE = 0.64). LUI_{500m} was generally a better predictor of DIN (mean explained variance: 39.1 %, nRMSE = 0.81) than LUI_{100m} (mean explained variance: 9.9 %, RMSE = 0.79) or BUFF (mean explained variance: 6 %, nRMSE = 0.79). LUI_{500m} was generally a better predictor of SRP (mean explained variance: 9 %, nRMSE = 1.50) than LUI_{100m} (mean explained variance: 6 %, nRMSE = 1.54), BUFF (mean explained variance: 5 %, nRMSE = 1.54) or $NDVI_{100m}$ (mean explained variance: 2 %, nRMSE = 1.58).

3.2. Remote sensing versus instream conditions to predict macrophyte biomass

The riparian vegetation density ($NDVI_{100m}$) showed negative associations with aquatic vascular plant biomass (mean standardized coefficient ± SE: −1.32 ± 0.20; Fig. 5a) together with the riparian forest buffer widths (BUFF; mean standardized coefficient ± SE: −0.51 ± 0.13). Conversely, the land use intensification index at reach scale (LUI_{100m}) showed positive associations with aquatic vascular plant biomass (mean standardized coefficient ± SE: 1.2 ± 0.26) together with the land use intensification index at segment scale (LUI_{500m}; mean standardized coefficient ± SE: −1.07 ± 0.29). Although weakly (weight ≤ 0.08), channel shading generally showed negative associations with aquatic vascular plant biomass (mean standardized coefficient ± SE: −0.62 ± 0.02). DIN also showed negative associations with vascular plant biomass (mean standardized coefficient ± SE: 1.1 ± 0.14). The best predictors (Fig. 5b) for aquatic vascular plant biomass were riparian density $NDVI_{100m}$ (mean explained variance: 16.4 %), followed by LUI_{100m} (mean explained variance: 4.9 %), BUFF (mean explained variance: 2.7 %) and DIN (mean explained variance: 2.2 %).

The habitat heterogeneity index showed positive associations with bryophyte biomass (mean standardized coefficient ± SE: 0.83 ± 0.15; Fig. 6a). Conversely, the percentage of fine sediments showed negative associations with bryophyte biomass (mean standardized coefficient ± SE: −0.67 ± 0.23) together with the river width (mean standardized coefficient ± SE: −0.29 ± 0.02). Remote sensing metrics showed poor capacity to predict bryophyte biomass. The best predictors (Fig. 6b) for bryophyte biomass were the habitat heterogeneity index (mean explained variance: 13.3 %), followed by percentage of fine sediments (mean explained variance: 4.3 %) and channel width (mean explained variance: 1.1 %).

4. Discussion

Our results showed that remote sensing information based on Sentinel-2 and the latest freely available data can be used to support the assessment of riparian and river ecosystem health. This differs from conclusion in previous studies (Dias-Silva et al., 2021), probably due to the way in which remote sensing metrics were derived. For example, in our study we used Sentinel-2 products with higher spatial resolution (10 m per pixel) comparing to Landsat 5 TM (30 m per pixel) used by Dias-Silva et al. (2021). Considering the high spatial heterogeneity of river landscape, the use of the new generation of satellites (e.g., Sentinel-2, Planet and Worldview), with higher spatial resolution, can be crucial for retrieving more accurate remote sensing indicators for the characterization of the riparian vegetation structure and complexity (Phiri et al., 2020; Cavender-Bares et al., 2022). The increasing use of high-resolution satellite-based indicators will extend our understanding to a much larger scale, allowing water managers to better keep track of all components of the water basins in river landscape (McVicar et al., 2017; Nagler et al., 2020).

In our study area, the combination of the riparian forest buffer width

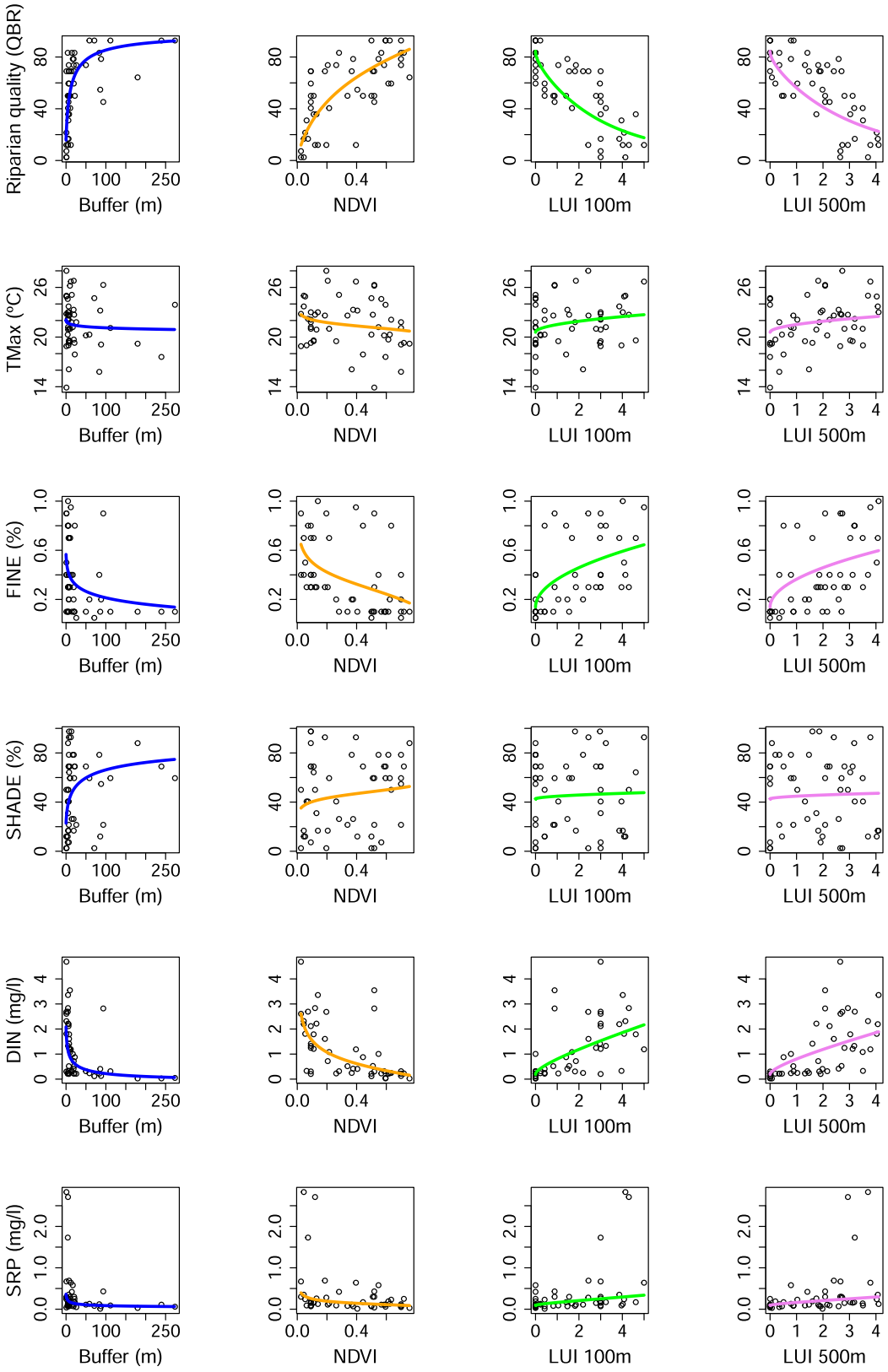

Fig. 3. Relationships between remote sensing variables and riparian quality or instream conditions. Buff: riparian forest buffer widths, NDVI: riparian density within 100 × 100 m cell; LUI100m: Land Use Index within 100 × 100 m cell; LUI500m = Land Use intensification index within 500 × 500 m cell, QBR: riparian quality index, TMax = maximum daily temperature; FINE: percentage of fine sediments; SHADE: percentage of stream channel shading; DIN: dissolved inorganic nitrogen concentration; SRP: Soluble reactive phosphorus concentration). Pearson correlation coefficients between variables are in Table S2.

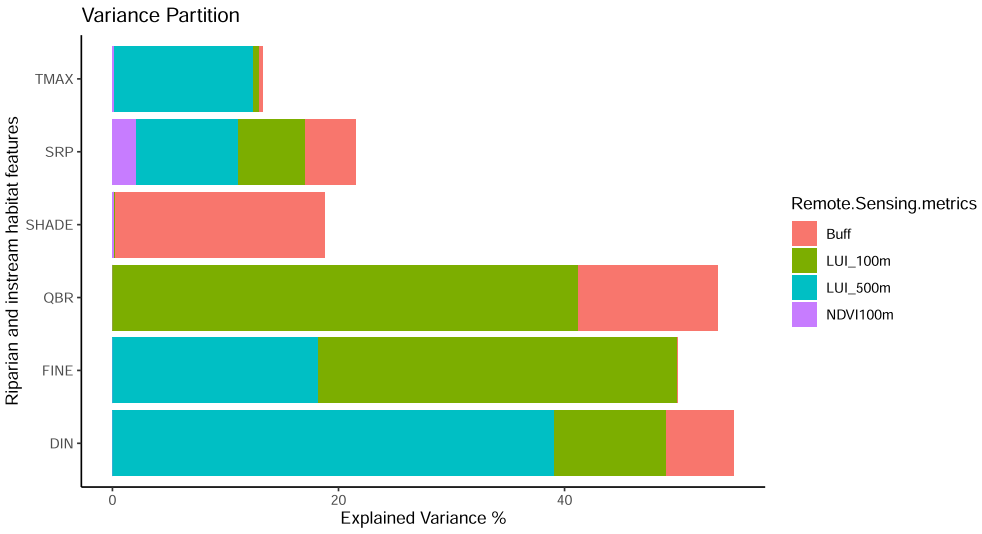

Fig. 4. Relative contribution of remote sensing metrics to explain riparian and instream conditions. Values represent weighted mean explained variances across retained models (ΔAICc ≤ 2) (Supporting information). Remote sensing metrics: Buff: riparian forest buffer widths, NDVI100m: riparian density within 100 × 100 m cell; LUI_100m: Land Use Intensification Index within 100 × 100 m cell; LUI_500m = Land Use index within 500 × 500 m cell. Riparian and instream habitat features: QBR: riparian quality index; Max Temp: maximum temperature within 24 h; FINE: percentage of fine sediments; Shadow: percentage of stream channel shading; DIN: dissolved inorganic nitrogen concentration; SRP: Soluble reactive phosphorus. Ranking of linear models between remote sensing variables and instream conditions are in Table S4. Results of 5-fold cross-validation process between remote sensing metrics and field measures (riparian and habitat features) are in Table S7.

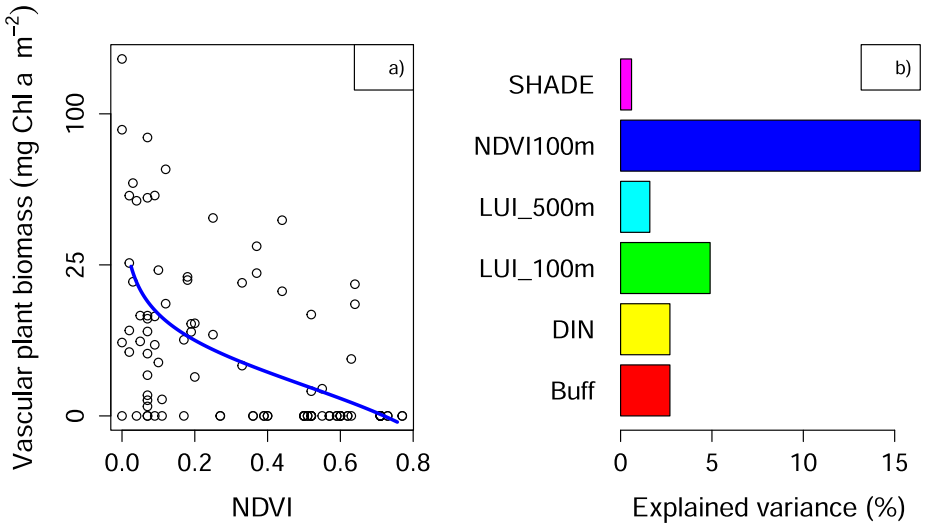

Fig. 5. (a) Relationship between riparian NDVI index and aquatic vascular plant biomass (mg Chl a m-2). (b) Relative contribution of predictors of aquatic vascular plant biomass. Values represent weighted mean explained variances across retained models (ΔAICc ≤ 2). (Buff = riparian forest buffer widths, NDVI100m = riparian density within 100 × 100 m cell; LUI100m = Land Use Intensification Index within 100 × 100 m cell; LUI500m = Land Use Intensification index within 500 × 500 m cell; SHADE = percentage of stream channel shading; DIN = dissolved inorganic nitrogen concentration concentration. Coefficient predictors for aquatic vascular plant biomass are in Table S5.

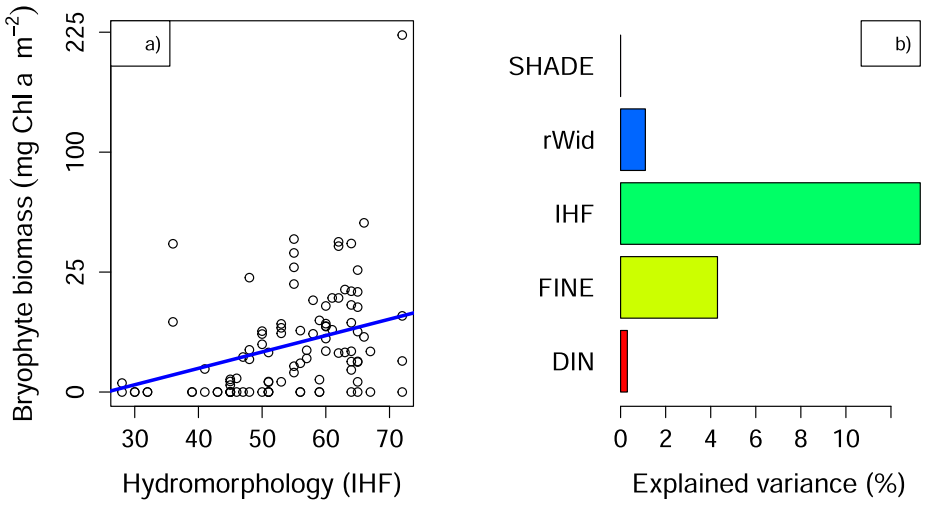

Fig. 6. (a) Relationship between the hydromorphology index and bryophyte biomass (mg Chl a m-2). (b) Relative contribution of predictors of bryophyte biomass. Values represent weighted mean explained variances across retained models (ΔAICc ≤ 2) (Supporting information). FINE: percentage of fine sediments; SHADE: percentage of stream channel shading; DIN = dissolved inorganic nitrogen concentration; IHF: habitat heterogeneity index; rWid = river width). Coefficient predictors for bryophyte biomass are in Table S6.

(r2 = 0.51 and nRMSE = 0.38, Table S7) and the land use intensification index at the reach scale (r2 = 0.60 and nRMSE = 0.34, Table S7) showed the highest power for predicting the riparian vegetation quality. The riparian forest buffer width, considers the size of the area where hydrological and ecological processes and functions take place. Therefore, it is directly related to the amount of available natural habitat within the riparian zone (del Tánago and de Jalón, 2006; Zaimes and Iakovoglou, 2021). For example, as the width of riparian buffer increases, shrubland and woodland become the main land use variables (Song et al., 2021). In contrast, the loss of riparian forest cover is particularly notable in anthropogenic landscapes (Turunen et al., 2021) and major changes in the structure and continuity of the riparian vegetation are usually observed in areas where a large expansion of agricultural activity exists (Latsiou et al., 2021). Thus, from a monitoring point of view, our findings support that remote sensing techniques can have an added value over the traditional field-based approaches used for the assessment of the riparian vegetation, but do not replace them (Huylenbroeck et al., 2020; Zaimes and Iakovoglou, 2021). Particularly, aerial images can be used for the assessment of generic riparian characteristics (e.g., width, continuity and connectivity), whereas land use information can assist to detect indirectly the major drivers of hydromorphological modifications within the riparian zone (e.g., bank and channel resectioning and reinforcement). However, field-based protocols still remain important for specific local assessment (e.g., severity) of anthropogenic impacts (e.g., garbage dumping, grazing, bank conditions, erosion and channel features).

Concerning stream water nutrients, we found that the combination of the riparian forest buffer width and the land use intensification index at segment scale (LUI_{500m}) has a high power for predicting DIN concentration. This was expected since measures of riparian buffer width reflect the ability of riparian lateral continuity to retain and transform nutrients and contaminants from terrestrial environments (Pärn et al., 2012; Weissteiner et al., 2014; Sweeney and Newbold, 2014). Buffer zones composed of forest trees show a higher nutrient removal rate compared with areas of grass and shrub vegetation (Aguiar et al., 2015). For these reasons, planting trees either as buffers/riparian forests or replacing agricultural areas is increasingly considered an effective measure to enhance river ecosystem functions and services by contributing, for instance, to nutrient retention and soil erosion control (Feld et al. 2018). This opens new opportunities to implement incentive-based policies for achieving environmental goals, namely the creation of cost-effective instruments for payments for ecosystem services (Valatin et al., 2022). In addition, we suggest to integrate the buffer width information with the land use intensification index at the segment scale (LUI_{500m}), since this index may add an indication of the nutrient loads in the area. Indeed, highest concentrations of water nutrients are usually observed in streams draining small catchments with high intensity of agriculture or urban land (Jarvie et al., 2010; Song et al., 2020). Surprisingly, we found a limited capacity to predict the concentrations of soluble reactive phosphorus (SRP) comparing to DIN.

One possible explanation is related to the way nutrients enter in the water. On one hand, nitrogen is highly soluble and mobile and is often transported into river systems via subsurface flow paths (Weigelhofer et al., 2018). By contrast, SRP easily adsorbs to charged soil particles, and enter mainly via soil erosion (Withers and Jarvie, 2008). In this sense, soil features may play a key role in phosphorous retention that can limit our prediction ability. Thus, to increase the model accuracy for SRP, future modes should incorporate soil properties (e.g., granulometry, infiltration, erodibility).

Land use intensification indices, at both reach and segment scale (LUI_{100m} and LUI_{500m}), were also correlated to the percentage of instream fine sediments. This can be expected since land-use properties and practices (e.g., substitution of natural vegetation patches by agriculture or pastures) have been often identified as drivers of natural fine sediment intrusion (e.g., Allan, 2004; Donovan and Monaghan, 2021). Considering that vegetation in the stream banks contributes to stream bank stability (Krzeminska et al., 2019), anthropogenic disturbances (e.g., the removal of riparian vegetation) can lead to higher bank erosion affecting fine sediment dynamics, with negative impacts on river ecosystems (Hauer et al., 2018). However, in our study we did not analyse the stream bank erosion at the reach scale, so such hypothesis needs to be confirmed in further research.

One of the main novelties of this study is that we found that the riparian vegetation density, assessed by NDVI, was a good predictor only for aquatic vascular plant biomass. The riparian vegetation density reflects both the structure and the phenology of the vegetation close to the water channel. Considering that riparian forests and shrubs on the river banks increase shading (Hrivnák et al., 2010), the riparian vegetation density can act as a proxy of light input, particularly in small forest streams (Garner et al., 2017; Savoy et al., 2021). This explains the high predictive power for aquatic vascular plant biomass in our study, also taking into account that light is considered the main limiting factor for photosynthesis and critical for the distribution of macrophyte community (Jusik and Staniszewski, 2019). Among aquatic vascular plants, amphiphytes, typical helophytes (i.e., emergent species) and graminoids, are favored in open habitats and shallow littoral zones with minimum shading (Hrivnák et al., 2010; Turunen et al., 2021), which was the case in our study.

However, considering the pivotal role of riparian vegetation in regulating thermal regimes and light inputs (Yirigui et al., 2019, Riis et al., 2020), we expected a stronger predictive power of the riparian vegetation density and the riparian forest buffer width for the maximum water temperature and the percentage of stream channel shading. One potential reason is that key factors, such as topography (e.g., channel orientation) and geomorphological characteristics (e.g., river type, stream width, channel features), were not included in our predictive models. For instance, concerning water temperature, topography and channel features, such as the channel orientation or the banks incision, can limit the time period that streams receive radiation inputs (Yard et al., 2005). In addition, light may be further attenuated by changes in water depth or clarity (Julian et al., 2013). Therefore, channel features, water depth and transparency can affect water temperature and should be considered in future studies. Concerning the percentage of stream channel shading, a minimum buffer width for sufficient shading would depend on stream orientation, differing from east–west, north–south orientated to meandering rivers (DeWalle, 2010). Also, the ratio of canopy height to stream width has been reported as a factor with high influence on stream channel shading (Kalny et al., 2017).

Finally, we showed a stronger association between bryophyte biomass and local abiotic variables (habitat heterogeneity and percentage of fine sediments) compared to remote sensing metrics. Indeed, sediments act as an anchoring substrate and source of nutrients for aquatic macrophytes that vary in their preference for sediment quality and type (Lacoul and Freedman, 2006). For example, aquatic bryophytes (e.g. *Fontinalis* spp. and *Hygrohypnum ocraceum)* may dominate mountain streams with abundant large boulders (Cattaneo and Fortin, 2000). Therefore, increasing sedimentation from forest management practices (e.g., due to logging and clearcutting) can be considered a key stressor inducing the loss of bryophyte biomass (Turunen et al., 2020) observed in our study. In this case, predicting bryophyte biomass requires in-channel features, such as channel substrate type (e.g., boulders and cobbles) and habitat heterogeneity. Such features are generally difficult to detect using remote sensing, based on satellite information, due to the physical properties of water and the related specificities of the electromagnetic radiation's reflection (Knehtl et al., 2018). Therefore, to bridge the existing scale gap, we suggest to assess stress in small-stature vegetation using ultra-high spatial resolution imagery (pixel size < 10 cm) derived from unmanned aircraft systems (Husson et al., 2014; Malenovský et al., 2017). However, in small rivers, and especially when the riparian vegetation is too dense, the use of unmanned aircraft systems cannot provide adequate information.

For these reasons, the monitoring of physical habitat parameters

(substrata and habitat heterogeneity), based on field protocols, continues to play an important and indispensable role in river health assessment.

5. Conclusion

Our results can be particularly important for environmental managers that need information about entire river networks to quickly detect 'hotspots' of anthropogenic pressures. Although, our study represents a first step to develop predictive models, it provides relevant insights on how a large and suitable asset of decision support information can be generated from the freely available remote sensing data helping to detect impacts on quality elements commonly used in river biomonitoring and to identify critical areas within river basins. Future efforts should test the predictive capacity of remote sensing metrics over larger spatio-temporal scales to reinforce the empirical support of our findings.

However, we recognize that *in situ* measurements, with particular focus on banks (e.g., stability and erosions), and channel condition (e.g., substrate type and heterogeneity) are still needed to complement the overall view derived from satellite-based indicators and to get a more detailed picture of the local impacts. In addition, *in situ* measurements would be recommended when satellite indicators show values for concern, with the need to specify content and extent of damage.

In further research, considering the high revisit frequency of satellite-based data, the derived multi temporal indicators would provide interesting information for the analysis of riparian vegetation phenology and characteristics (e.g., presence of evergreen/deciduous species or presence of alien species), that would permit advances for the monitoring ecological processes under changing environmental or hydroclimatic conditions and for the development of early warnings systems.

CRediT authorship contribution statement

G. Pace: Conceptualization, Data curation, Formal analysis, Methodology, Writing – original draft, Writing – review & editing. **C. Gutiérrez-Cánovas:** Conceptualization, Data curation, Formal analysis, Methodology, Writing – original draft, Writing – review & editing. **R. Henriques:** Conceptualization, Data curation, Methodology, Supervision, Writing – review & editing. **C. Carvalho-Santos:** Conceptualization, Writing – original draft, Writing – review & editing. **F. Cássio:** Conceptualization, Supervision, Writing – review & editing. **C. Pascoal:** Conceptualization, Supervision, Writing – original draft, Writing – review & editing.

Declaration of Competing Interest

The authors declare that they have no known competing financial interests or personal relationships that could have appeared to influence the work reported in this paper.

Data availability

The data that has been used is confidential.

Acknowledgements

The authors would like to thank the anonymous reviewers and the editor for their insightful comments.

This work was supported by the River2Ocean project (NORTE-01-0145- FEDER-000068), co-financed by the European Regional Development Fund (ERDF), through Programa Operacional Regional do Norte (NORTE 2020).

The work was also supported by the "Contrato-Programa" UIDB/04050/2020 funded by national funds through the FCT I.P., the Centre of Molecular and Environmental Biology (CBMA). CG-C was supported by a "Juan de la Cierva – Incoporación" contract (MINECO, IJC2018-036642-I). CCS was supported by the "Financiamento Programático" UIDP/04050/2020 funded by national funds through the FCT I.P.

Appendix A. Supplementary data

Supplementary data to this article can be found online at https://doi.org/10.1016/j.ecolind.2022.109519.

References

Aguiar, J.T.R., Rasera, K., Parron, L.M., Brito, A.G., Ferreira, M.T., 2015. Nutrient removal effectiveness by riparian buffer zones in rural temperate watersheds: the impact of no-till crops practices. Agric. Water Manag.e. 149, 74–80. https://doi.org/10.1016/j.agwat.2014.10.031.

Allan, J.D., 2004. Landscapes and riverscapes: the influence of land use on stream ecosystems. Annu. Rev. Ecol. Evol. Syst. 35, 257–284. https://doi.org/10.1146/ANNUREV.ECOLSYS.35.120202.110122.

Álvarez-Martínez, J.M., Jiménez-Alfaro, B., Barquín, J., Ondiviela, B., Recio, M., Silió-Calzada, A., Juanes, J.A., Isaac, N., 2018. Modelling the area of occupancy of habitat types with remote sensing. Methods Ecol. Evol. 9 (3), 580–593.

Araujo, M., Valério, P., Jouanneau, J., 1998. Heavy metal assessment in sediments of the ave river basin by energy-dispersive (Portugal) X-Ray Fluorescence Spectrometry. X-Ray Spectrom. 27, 305–312. https://doi.org/10.1002/(SICI)1097-4539(199809/10)27:5<305::AID-XRS275>3.0.CO;2-7.

Baattrup-Pedersen, A., Szoszkiewicz, K., Nijboer, R., O'Hare, M., Ferreira, T., 2006. Macrophyte communities in unimpacted European streams: variability in assemblage patterns, abundance and diversity. Hydrobiologia 566, 179–196. https://doi.org/10.1007/978-1-4020-5493-8_13.

Barton, K., 2020. *MuMIn: multi-model inference. – R package ver. 1.43.17* Available at: https://cran.r-project.org/web/packages/MuMIn/ index.html (Accessed 11 May 2022).

Birk, S., Chapman, D., Carvalho, L., Spears, B.M., Andersen, H.E., Argillier, C., Auer, S., Baattrup-Pedersen, A., Banin, L., Beklioğlu, M., Bondar-Kunze, E., Borja, A., Branco, P., Bucak, T., Buijse, A.D., Cardoso, A.C., Couture, R.-M., Cremona, F., de Zwart, D., Feld, C.K., Ferreira, M.T., Feuchtmayr, H., Gessner, M.O., Gieswein, A., Globevnik, L., Graeber, D., Graf, W., Gutiérrez-Cánovas, C., Hanganu, J., Işkın, U., Järvinen, M., Jeppesen, E., Kotamäki, N., Kuijper, M., Lemm, J.U., Lu, S., Solheim, A. L., Mischke, U., Moe, S.J., Nõges, P., Nõges, T., Ormerod, S.J., Panagopoulos, Y., Phillips, G., Posthuma, L., Pouso, S., Prudhomme, C., Rankinen, K., Rasmussen, J.J., Richardson, J., Sagouis, A., Santos, J.M., Schäfer, R.B., Schinegger, R., Schmutz, S., Schneider, S.C., Schülting, L., Segurado, P., Stefanidis, K., Sures, B., Thackeray, S.J., Turunen, J., Uyarra, M.C., Venohr, M., von der Ohe, P.C., Willby, N., Hering, D., 2020. Impacts of multiple stressors on freshwater biota across spatial scales and ecosystems. Nat. Ecol. Evol. 4 (8), 1060–1068.

Bizzi, S., Demarchi, L., Grabowski, R.C., Weissteiner, C.J., Van de Bund, W., 2016. The use of remote sensing to characterise hydromorphological properties of European rivers. Aquat. Sci. 78, 57–70. https://doi.org/10.1007/s00027-015-0430-7.

Bruno, D., Gutiérrez-Cánovas, C., Sánchez-Fernández, D., Velasco, J., Nilsson, C., Li, J.-T., 2016. Impacts of environmental filters on functional redundancy in riparian vegetation. J. Appl. Ecol. 53 (3), 846–855.

Burnham, K.P., Anderson, D.R., 2002. Model Selection and Multimodel Inference: A Practical Information-Theoretic Approach 2nd ed. Springer, New York (NY) 10.1007/b97636 978–0-387-95364-9.

Capon, S.J., Stewart-Koster, B., Bunn, S.E., 2021. Future of freshwater ecosystems in a 1.5°C warmer world. Front. Environ. Sci. 9 (784642) https://doi.org/10.3389/fenvs.2021.784642.

Carvalho, L., Mackay, E.B., Cardoso, A.C., Baattrup-Pedersen, A., Birk, S., Blackstock, K. L., Borics, G., Borja, A., Feld, C.K., Ferreira, M.T., Globevnik, L., Grizzetti, B., Hendry, S., Hering, D., Kelly, M., Langaas, S., Meissner, K., Panagopoulos, Y., Penning, E., Rouillard, J., Sabater, S., Schmedtje, U., Spears, B.M., Venohr, M., van de Bund, W., Solheim, A.L., 2019. Protecting and restoring Europe's waters: An analysis of the future development needs of the Water Framework Directive. Sci. Total Environ. 658, 1228–1238.

Cattaneo, A., Fortin, L., 2000. Moss distribution in streams of the Quebec Laurentian Mountains. Can. J. Bot. 78, 748–752. https://doi.org/10.1139/b00-050.

Cavender-Bares, J., Schneider, F.D., Santos, M.J., Armstrong, A., Carnaval, A., Dahlin, K. M., Fatoyinbo, L., Hurtt, G.C., Schimel, D., Townsend, P.A., Ustin, S.L., Wang, Z., Wilson, A.M., 2022. Integrating remote sensing with ecology and evolution to advance biodiversity conservation. Nat. Ecol. Evol. 6 (5), 506–519.

Costa, H., Almeida, D., Vala, F., Marcelino, F., Caetano, M., 2018. Land Cover Mapping from Remotely Sensed and Auxiliary Data for Harmonized Official Statistics. ISPRS Int. J. Geo-Inf. 7, 157. https://doi.org/10.3390/ijgi7040157.

De Sosa, L.L., Glanville, H.C., Marshall, M.R., Abood, S.A., Williams, A.P., Jones, D.L., 2018. Delineating and mapping riparian areas for ecosystem service assessment. Ecohydrology 11 (2), e1928.

del Tánago, M.G., de Jalón, D.G., 2006. Attributes for assessing the environmental quality of riparian zones. Limnetica 25, 389–402. https://doi.org/10.23818/limn.25.27.

DeWalle, D.R., 2010. Modeling stream shade: riparian buffer height and density as important as buffer width. J. Am. Water Resour. Assoc. 46, 323–333.

Dias-Silva, K., Vieira, T.B., de Matos, T.P., Juen, L., Simião-Ferreira, J., Hughes, R.M., De Marco Júnior, P., 2021. Measuring stream habitat conditions: Can remote sensing substitute for field data? Sci. Total Environ. 788, 147617.
Donovan, M., Monaghan, R., 2021. Impacts of grazing on ground cover, soil physical properties and soil loss via surface erosion: a novel geospatial modelling approach. J. Environ. Manage. 287, 112206.
Doody, T.M., Lewis, M., Benyon, R.G., Byrne, G., 2014. A method to map riparian exotic vegetation (Salix spp.) area to inform water resource management. Hydrol. Process. 28, 3809–3823. https://doi.org/10.1002/hyp.9916.
Dudgeon, D., Arthington, A.H., Gessner, M.O., Kawabata, Z.-I., Knowler, D.J., Lévêque, C., Naiman, R.J., Prieur-Richard, A.-H., Soto, D., Stiassny, M.L.J., Sullivan, C.A., 2006. Freshwater biodiversity: importance, threats, status and conservation challenges. Biol. Rev. 81 (02), 163.
EEA, 2018. European waters – assessment of status and pressures 2018. EEA Report 7/, 2018.
Erba, S., Pace, G., Demartini, D., Di Pasquale, D., Dorflinger, G., Buffagni, A., 2015. Land use at the reach scale as a major determinant for benthic invertebrate community in Mediterranean rivers of Cyprus. Ecol. Ind. 48, 477–491. https://doi.org/10.1016/j.ecolind.2014.09.010.
EC European Commission, 1992. Council Directive 92/43/EEC of 21 May 1992 on the conservation of natural habitats and of wild fauna and flora. Official Journal L 7–50 (22 July 1992).
EC European Commission, 2013. Interpretation Manual of European Union Habitats – EUR28. European Commission, DG Environment, p. 144 Nature ENV B.3.
Evangelista, H.B., Michelan, T.S., Gomes, L.C., Thomaz, S.M., Souza, L., 2017. Shade provided by riparian plants and biotic resistance by macrophytes reduce the establishment of an invasive Poaceae. J. Appl. Ecol. 54 (2), 648–656.
Feld, C.K., 2004. Identification and measure of hydromorphological degradation in Central European lowland streams. Hydrobiologia 516, 69–94. https://doi.org/10.1023/B:HYDR.0000025259.01054.f2.
Feld, C.K., Fernandes, M.R., Ferreira, M.T., Hering, D., Ormerod, S.J., Venohr, M., Gutiérrez-Cánovas, C., 2018. Evaluating riparian solutions to multiple stressor problems in river ecosystems — a conceptual study. Water Res. 139, 381–394.
Fernandes, M.R., Aguiar, F.C., Ferreira, M.T., 2011. Assessing riparian vegetation structure and the influence of land use using landscape metrics and geostatistical tools. Landscape Urban Plann. 99, 166–177. https://doi.org/10.1016/j.landurbplan.2010.11.001.
Filipe, A.F., Feio, M.J., Garcia-Raventós, A., Ramião, J.P., Pace, G., Martins, F.MS., Magalhães, M.F., 2019. The European water framework directive facing current challenges: recommendations for a more efficient biological assessment of inland surface waters. Inland Waters 9 (1), 95–103.
Finkler, N.R., Gücker, B., Boëchat, I.G., Ferreira, M.S., Tanaka, M.O., Cunha, D.G.F., 2021. Riparian land use and hydrological connectivity influence nutrient retention in tropical rivers receiving wastewater treatment plant discharge. Front. Environ. Sci. 9, 709922 https://doi.org/10.3389/fenvs.2021.709922.
Fonseca, A., Ugille, J.P., Michez, A., Rodríguez-González, P.M., Duarte, G., Ferreira, M. T., Fernandes, M.R., 2021. Assessing the connectivity of riparian forests across a gradient of human disturbance: the potential of copernicus "riparian zones" in two hydroregions. Forests 12, 674. https://doi.org/10.3390/f12060674.
Garner, G., Malcolm, I.A., Sadler, J.P., Hannah, D.H., 2017. The role of riparian vegetation density, channel orientation and water velocity in determining river temperature dynamics. J. Hydrol. 553, 471–485. https://doi.org/10.1016/j.jhydrol.2017.03.024.
Grueber, C.E., Nakagawa, S., Laws, R.J., Jamieson, I.G., 2011. Multimodel inference in ecology and evolution: challenges and solutions. J. Evol. Byol. 24, 699–711. https://doi.org/10.1111/j.14420-9101.2010.02210.
Gurnell, A.M., Petts, G.E., Hannah, D.M., Smith, B.P.G., Edwards, P.J., Kollman, J., Ward, J.V., Tockner, C., 2001. Riparian vegetation and island formation along the gravel bed Fiume Tagliamento, Italy. Earth Surf. Process. Land. 26, 31–62. https://doi.org/10.1002/1096-9837(200101)26:1<31::AID-ESP155>3.0.CO;2-Y.
Hauer, C., Leitner, P., Unfer, G., Pulg, U., Habersack, H., Graf, W., 2018. The Role of Sediment and Sediment Dynamics in the Aquatic Environment Pages 151-169 in S. Schmutz and J.Sendzimir (Eds) *Riverine Ecosystem Management.* Aquatic Ecology Series 8, Springer, Cham DOI:10.1007/978-3-319-73250-3_10.
Hoffman, G.E., Schadt, E.E., 2016. variancePartition: interpreting drivers of variation in complex gene expression studies. BMC Bioinf. 17, 483. https://doi.org/10.1186/s12859-016-1323-z.
Holloway, J., Mengersen, K., 2018. Statistical machine learning methods and remote sensing for sustainable development goals: a review. Remote Sens. 10, 1365. https://doi.org/10.3390/rs10091365.
Hrivnák, R., Ot'ahel'ová, H., Valachovič, M., Pal'ove-Balang, P., Kubinská, A., 2010. Effect of environmental variables on the aquatic macrophyte composition pattern in streams: a case study from Slovakia. Fundam. Appl. Limnol. 177 (2), 115–124.
Husson, E., Hagner, O., Ecke, F., Schmidtlein, S., 2014. Unmanned aircraft systems help to map aquatic vegetation. Appl. Veg. Sci. 17 (3), 567–577.
Huylenbroeck, L., Laslier, M., Dufour, S., Georges, B., Lejeune, P., Michez, A., 2020. Using remote sensing to characterize riparian vegetation: a review of available tools and perspectives for managers. J. Environ. Manage. 267, 110652 https://doi.org/10.1016/j.jenvman.2020.110652.
INAG, 2008. Manual para a avaliação biológica da qualidade da água em sistemas fluviais segundo a Directiva-Quadro da Água - Protocolo de amostragem e análise para os macrófitos. Ministério do Ambiente, do Ordenamento do Território e do Desenvolvimento Regional. Instituto da Água, I.P.
Jarvie, H.P., Withers, P.J.A., Bowes, M.J., Palmer-Felgate, E.J., Harper, D.M., Wasiak, K., Wasiak, P., Hodgkinson, R.A., Bates, A., Stoate, C., Neal, M., Wickham, H.D., Harman, S.A., Armstrong, L.K., 2010. Streamwater phosphorus and nitrogen across a gradient in rural-agricultural land use intensity. Agric. Ecosyst. Environ. 135 (4), 238–252.
Jeffrey, S.W., Humphrey, G.F., 1975. New spectrophotometric equations for determining chlorophylls a, b, c1 and c2 in higher plants, algae and natural phytoplankton. Biochem. Physiol. Pflanz 167, 191–194. https://doi.org/10.1016/S0015-3796(17)30778-3.
Julian, J.P., Davies-Colley, R.J., Gallegos, C.L., Tran, T.V., 2013. Optical water quality of inland waters: a landscape perspective. Ann. Assoc. Am. Geogr. 103 (2), 309–318.
Jusik, S., Staniszewski, R., 2019. Shading of river channels as an important factor reducing macrophyte biodiversity. Pol. J. Environ. Stud. 28, 1215–1222. https://doi.org/10.15244/pjoes/81559.
Kalny, G., Laaha, G., Melcher, A., Trimmel, H., Weihs, P., Rauch, H.P., 2017. The influence of riparian vegetation shading on water temperature during low flow conditions in a medium sized river. Knowl. Manag. Aquat. Ecosyst. 418, 5. https://doi.org/10.1051/kmae/2016037.
Knehtl, M., Petkovska, V., Urbanič, G., 2018. Is it time to eliminate field surveys from hydromorphological assessments of rivers? - Comparison between a field survey and a remote sensing approach. Ecohydrology 11 (2). https://doi.org/10.1002/eco.1924.
Krzeminska, D., Kerkhof, T., Skaalsveen, K., Stolte, J., 2019. Effect of riparian vegetation on stream bank stability in small agricultural catchments. CATENA 172, 87–96. https://doi.org/10.1016/j.catena.2018.08.014.
Lacoul, P., Freedman, B., 2006. Environmental influences on aquatic plants in freshwater ecosystems. Environ. Rev. 14, 89–136. https://doi.org/10.1139/a06-001.
Latsiou, A., Kouvarda, T., Stefanidis, K., Papaioannou, G., Gritzalis, K., Dimitriou, E., 2021. Pressures and Status of the Riparian Vegetation in Greek Rivers: overview and Preliminary Assessment. Hydrology 8, 55. https://doi.org/10.3390/hydrology8010055.
Lei, C., Wagner, P.D., Fohrer, N., 2021. Effects of land cover, topography, and soil on stream water quality at multiple spatial and seasonal scales in a German lowland catchment. Ecol. Ind. 120, 106940 https://doi.org/10.1016/j.ecolind.2020.106940.
Malenovský, Z., Lucieer, A., King, D.H., Turnbull, J.D., Robinson, S.A., Lecomte, N., 2017. Unmanned aircraft system advances health mapping of fragile polar vegetation. Methods Ecol. Evol. 8 (12), 1842–1857.
McVicar, T.M., Van Niel, T.G., Li L. 2017. Remote sensing of land-use-specific actual evapotranspiration of entire catchments containing plantations. Scientific Report. ISBN: 978-1-925213-60-7. Forest & Wood Products Australia.
Michez, A., Piégay, H., Lejeune, P., Claessens, H., 2017. Multi-temporal monitoring of a regional riparian buffer network (>12,000 km) with LiDAR and photogrammetric point clouds. J. Environ. Manage. 202, 424–436. https://doi.org/10.1016/j.jenvman.2017.02.034.
Monteagudo, L., Moreno, J.L., Picazo, F., 2012. River eutrophication: irrigated vs. non-irrigated agriculture through different spatial scales. Water Res. 46, 2759–2771. https://doi.org/10.1016/j.watres.2012.02.035.
Mota, M., Sousa, R., Bio, A., Araujo, M.J., Braga, C., Antunes, C., 2014. Seasonal changes in fish assemblages in the River Minho tidal freshwater wetlands, NW of the Iberian Peninsula. Ann. Limnol. Int. J. Lim. 50, 185–198. https://doi.org/10.1051/limn/2014012.
Munné, A., Prat, N., Solà, C., Bonada, N., Rieradevall, M., 2003. A simple field method for assessing the ecological quality of riparian habitat in rivers and streams: QBR index. Aquat. Conserv. Mar. Freshwater Ecosyst. 13, 141–163. https://doi.org/10.1002/aqc.529.
Nagler, P.L., Doody, T.M., Glenn, E.P., Jarchow, C.J., Barreto-Muñoz, A., Didan, K., 2016. Wide-area estimates of evapotranspiration by red gum (Eucalyptus camaldulensis) and associated vegetation in the Murray– Darling River Basin, Australia. Hydrol. Process. 30, 1376–1387. https://doi.org/10.1002/hyp.10734.
Nagler, P.L., Barreto-Muñoz, A., Borujeni, S.C., Jarchow, C.J., Gómez-Sapiens, M.M., Nouri, H., Herrmann, S.M., Didan, K., 2020. Ecoohydrological responses to surface flow across borders: Two decades of changes in vegetation greenness and water use in the riparian corridor of the Colorado River delta. Hydrol. Process. 34, 4851–4883. https://doi.org/10.1002/hyp.13911.
Novillo, C.J., Arrogante-Funes, P., Romero-Calcerrada, R., 2019. Recent NDVI trends in mainland Spain: land-cover and phytoclimatic-type implications. ISPRS Int. J. GeoInf. 8, 43. https://doi.org/10.3390/ijgi8010043.
Pace, G., Gutiérrez-Cánovas, C., Henriques, R., Boeing, F., Cássio, F., Pascoal, C., 2021. Remote sensing depicts riparian vegetation responses to water stress in a humid Atlantic region. Sci. Total Environ. 772, 145526 https://doi.org/10.1016/j.scitotenv.2021.145526.
Pardo, I., Álvarez, M., Casas, J., Moreno, J.L., Vivas, S., Bonda, N., et al., 2002. El hábitat de los ríos mediterráneos. Diseño de un índice de diversidad de hábitat. Limnetica 21, 115–133.
Pärn, J., Pinay, G., Mander, Ü., 2012. Indicators of nutrients transport from agricultural catchments under temperate climate: a review. Ecol. Ind. 22, 4–15. https://doi.org/10.1016/j.ecolind.2011.10.002.
Partners, P., 2019. lmvar: Linear Regression with Non-Constant Variances. – R package ver. 1.5.2 Available at: https://cran.r-project.org/web/packages/lmvar/lmvar.pdf (Accessed 09 September 2022).
Peng, J., Liu, Z., Liu, Y., Wu, J., Han, Y., 2012. Trend analysis of vegetation dynamics in Qinghai—Tibet Plateau using Hurst Exponent. Ecol. Ind. 14, 28–39. https://doi.org/10.1016/J.ECOLIND.2011.08.011.
Pérez-Silos, I., Álvarez-Martínez, J.M., Barquín, J., Rocchini, D., 2019. Modelling riparian forest distribution and composition to entire river networks. Appl. Veg. Sci. 22 (4), 508–521.
Phiri, D., Simwanda, M., Salekin, S., Nyirenda, V.R., Muayama, Y., Ranagalage, M., 2020. Sentinel-2 data for land cover/use mapping: a review. Remote Sens. 12, 2291. https://doi.org/10.3390/rs12142291.

Potapov, P.V., Turubanova, S.A., Tyukavina, A., Krylov, A.M., McCarty, J.L., Radeloff, V. C., Hansen, M.C., 2015. Eastern Europe's forest cover dynamics from 1985 to 2012 quantified from the full landsat archive. Remote Sens. Environ. 159, 28–43.
Quantum GIS Development Team QGIS Geographic Information System Open Source Geospatial Foundation 2009 Available at: http://qgis.org. (Accessed 10 May 2022).
R Core Team R: A language and environment for statistical computing 2020 R Foundation for Statistical Computing Vienna, Austria https://www.R-project.org/. (Accessed 10 May 2022.
Rääpysjärvi, J., Hämäläinen, H., Aroviita, J., 2016. Macrophytes in boreal streams: characterizing and predicting native occurrence and abundance to assess human impact. Ecol. Ind. 64, 309–318. https://doi.org/10.1016/j.ecolind.2016.01.014.
Reid, A.J., Carlson, A.K., Creed, I.F., Eliason, E.J., Gell, P.A., Johnson, P.T.J., Kidd, K.A., MacCormack, T.J., Olden, J.D., Ormerod, S.J., Smol, J.P., Taylor, W.W., Tockner, K., Vermaire, J.C., Dudgeon, D., Cooke, S.J., 2019. Emerging threats and persistent conservation challenges for freshwater biodiversity. Biol. Rev. 94 (3), 849–873.
Riis, T., Kelly-Quinn, M., Aguiar, F.C., Manolaki, P., Bruno, D., Bejarano, M.D., Clerici, N., Fernandes, M.R., Franco, J.C., Pettit, N., Portela, A.P., Tammeorg, O., Tammeorg, P., Rodríguez-González, P.M., Dufour, S., 2020. Global overview of ecosystem services provided by riparian vegetation. Bioscience 70 (6), 501–514.
Rocchini, D., Luque, S., Pettorelli, N., Bastin, L., Doktor, D., Faedi, N., Feilhauer, H., Féret, J.-B., Foody, G.M., Gavish, Y., Godinho, S., Kunin, W.E., Lausch, A., Leitão, P. J., Marcantonio, M., Neteler, M., Ricotta, C., Schmidtlein, S., Vihervaara, P., Wegmann, M., Nagendra, H., Parrini, F., 2018. Measuring β-diversity by remote sensing: a challenge for biodiversity monitoring. Methods Ecol. Evol. 9 (8), 1787–1798.
Santos, J.M., Godinho, F., Ferreira, M.T., Cortes, R., 2004. The organisation of fish assemblages in the regulated Lima basin, Northern Portugal. Linmologica 34 (3), 224–235.
Savoy, P., Bernhardt, E., Kirk, L., Cohen, M.J., Heffernan, J.B., 2021. A seasonally dynamic model of light at the stream surface. Freshwater Science 40, 286–301. https://doi.org/10.1086/714270.
Schulz, D., Yin, H., Tischbein, B., Verleysdonk, S., Adamou, R., Kumar, N., 2021. Land use mapping using Sentinel-1 and Sentinel-2 time series in a hetereogeneous landscape in Niger, Sahel. ISPRS J. Photogramm. Remote Sens. 178, 97–111. https://doi.org/10.1016/j.isprsjprs.2021.06.005.
Song, M., Jiang, Y., Liu, Q., Tian, Y., Liu, Y., Xu, X., Kang, M., 2021. Catchment versus riparian buffers: which land use spatial scales have the greatest ability to explain water quality changes in a typical temperate watershed? Water 13, 1758. https://doi.org/10.3390/w13131758.
Song, Y., Song, X., Shao, G., Hu, T., 2020. Effects of land use on stream water quality in the rapidly urbanized areas: a multiscale analysis. Water 12, 1123D. https://doi.org/10.3390/w12041123.
Sweeney, B.W., Newbold, J.D., 2014. Streamside forest buffer width needed to protect stream water quality, habitat, and organisms: a literature review. J. Am. Water Resour. Assoc. (JAWRA) 50, 560–584. https://doi.org/10.1111/jawr.12203.
Torresani, M., Rocchini, D., Sonnenschein, R., Zebisch, M., Marcantonio, M., Ricotta, C., Tonon, G., 2019. Estimating tree species diversity from space in an alpine conifer forest: the Rao's Q diversity index meets the spectral variation hypothesis. Ecol. Inf. 52, 26–34.
Tran, C.P., Bode, R.W., Smith, A.J., Kleppel, G.S., 2010. Land-use proximity as a basis for assessing stream water quality in New York State (USA). Ecol. Ind. 10, 727–733. https://doi.org/10.1016/j.ecolind.2009.12.002.
Tremp, H., 2007. Spatial and environmental effects on hydrophytic macrophyte occurrence in the Upper Rhine floodplain (Germany). Hydrobiologia 586, 167–177. https://doi.org/10.1007/s10750-007-0617-6.
Tufekcioglu, M., Schults, R.C., Isenhart, T.M., Kovar, J.L., Russell, J.R., 2020. Riparian land-use, stream morphology and streambank erosion within grazed pastures in Southern Iowa, USA: a catchment-wide perspective. Sustainability 12, 6461. https://doi.org/10.3390/su12166461.
Turunen, J., Muotka, T., Aroviita, J., 2020. Aquatic bryophytes play a key role in sediment-stressed boreal headwater streams. Hydrobiologia 847, 605–615. https://doi.org/10.1007/s10750-019-04124-w.
Turunen, J., Elbrecht, V., Steinke, D., Aroviita, J., 2021. Riparian forests can mitigate warming and ecological degradation of agricultural headwater streams. Freshw. Biol. 00, 1–14. https://doi.org/10.1111/fwb.13678.
Valatin, G., Ovando, P., Abildtrup, J., Accastello, C., Andreucci, M.B., Chikalanov, A., El Mokaddem, A., Garcia, S., Gonzalez-Sanchis, M., Gordillo, F., Kayacan, B., Little, D., Lyubenova, M., Nisbet, T., Paletto, A., Petucco, C., Termansen, M., Vasylyshyn, K., Vedel, S.E., Yousefpour, R., 2022. Approaches to cost-effectiveness of payments for tree planting and forest management for water quality services. Ecosyst. Serv. 53, 101373.
Venter, Z.S., Sydenham, M.A.K., 2021. Continental-Scale Land Cover Mapping at 10 m Resolution over Europe (ELC10). Remote Sens. 13, 2301. https://doi.org/10.3390/rs13122301.
Vieira, J.M.P., Pinho, J.L.S., Duarte, A.A.L.S., 1998. Eutrophication vulnerability analysis: a case study. Water Sci. Technol. 37, 121–128. https://doi.org/10.1016/S0273-1223(98)00063-8.
Wahl, C., Neils, A., Hooper, D.U., 2013. Impacts of land use at the catchment scale constrain the habitat benefits of stream riparian buffers. Freshw. Biol. 58, 2310–2324. https://doi.org/10.1111/fwb.12211.
Wang, R., Gamon, J., Montgomery, R., Townsend, P., Zygielbaum, A., Bitan, K., Tilman, D., Cavender-Bares, J., 2016. Seasonal variation in the NDVI–species richness relationship in a prairie grassland experiment (Cedar Creek). Remote Sens. 8 (2), 128.
Weigelhofer, G., Hein, T., Bondar-Kunze, E., 2018. In: Riverine Ecosystem Management. Springer International Publishing, Cham, pp. 187–202.
Weissteiner, C.J., Pistocchi, A., Marinov, D., Bouraoui, F., Sala, S., 2014. An indicator to map diffuse chemical river pollution considering buffer capacity of riparian vegetation—a pan-European case study on pesticides. Sci. Total Environ. 484, 64–73. https://doi.org/10.1016/j.scitotenv.2014.02.124.
Withers, P.J.A., Jarvie, H.P., 2008. Delivery and cycling of phosphorus in rivers: a review. Sci. Total Environ. 400, 379–395. https://doi.org/10.1016/j.scitotenv.2008.08.002.
Yard, M.D., Bennett, G.E., Mietz, S.N., Coggins, L.G., Stevens, L.E., Hueftle, S., Blinn, D. W., 2005. Influence of topographic complexity on solar insolation estimates for the Colorado River, Grand Canyon, AZ. Ecol. Model. 183 (2-3), 157–172.
Yirigui, Y., Lee, S.-W., Nejadhashemi, A.P., Herman, M.R., Lee, J.-W., 2019. Relationships between Riparian Forest Fragmentation and Biological Indicators of Streams. Sustainability 11, 2870. https://doi.org/10.3390/su11102870.
Zaimes, G.N., Gounaridis, D., Symenonakis, E., 2019. Assessing the impact of dams on riparian and deltaic vegetation using remotely-sensed vegetation indices and Random Forests modelling. Ecol. Ind. 103, 630–641. https://doi.org/10.1016/j.ecolind.2019.04.047.
Zaimes, G.N., Iakovoglou, V., 2021. Assessing riparian areas of Greece—An overview. Sustainability 13, 309. https://doi.org/10.3390/su13010309.
Zuur, A.F., Ieno, E.N., Walker, N.J., Saveliev, A.A., Smith, G.M., 2009. *Mixed effects models and extensions in ecology with R.* – Springer.
Zuur, A.F., Ieno, E.N., Elphick, C.S., 2010. A protocol for data exploration to avoid common statistical problems. Methods Ecol. Evol. 1, 3–14. https://doi.org/10.1111/j.2041-210x.2009.00001.x.